Challenges of diagnosing glaucoma in myopic eyes

Qiu, Kunliang

Chapter 6

Characteristic pattern of OCT abnormalities in the RNFL thickness deviation map enables differentiation between false-positive and glaucoma in myopic eyes

Kunliang Qiu, Geng Wang, Riping Zhang, Xuehui Lu, Mingzhi Zhang, Nomdo M. Jansonius

Submitted

ABSTRACT

Aim: (1) To describe the pattern of OCT abnormalities in the peripapillary retinal nerve fiber layer (RNFL) deviation map in healthy myopic eyes and (2) to compare the location of the abnormalities between healthy and glaucomatous myopic eyes.

Methods: Peripapillary RNFL thickness was assessed with Cirrus OCT in 137 myopic eyes (median spherical equivalent -4.9 D) of 137 healthy subjects and 25 eyes (-4.6 D) of 25 glaucoma patients (Group 1) and with Topcon OCT-2000 in 116 myopic eyes (-3.0 D) of 116 healthy subjects and 74 eyes (-2.0 D) of 74 patients (Group 2). We recorded (1) the area of the color-coded region in the RNFL thickness deviation map and (2) the location of the color-coded region relative to the major temporal retinal vessels. We calculated the sensitivity and specificity with a positive test defined as (1) presence of a color-coded region that qualified as abnormal and (2) presence of a color-coded region that qualified as abnormal and was located at least partially on the temporal side of the major temporal vessels.

Results: By taking the location into account, the specificity increased from 22.6 to 96.4% in Group 1 ($P<0.001$) and from 62.1 to 94.0% in Group 2 ($P<0.001$). Corresponding sensitivities were 96 and 96% (Group 1) and 94.6 and 91.9% (Group 2).

Conclusions: The location of the color-coded region in the RNFL thickness deviation map relative to the major temporal retinal vessels offers a simple and valuable clue for differentiating between false-positive and glaucoma in myopic eyes.

Introduction

Glaucoma is a chronic and progressive eye disease characterized by loss of retinal ganglion cells (RGCs), thinning of the retinal nerve fiber layer (RNFL), and subsequent visual field loss. Optical coherence tomography (OCT) has enabled the in vivo measurement of RNFL thickness, which has been reported to be useful for glaucoma detection in clinical practice (Huang et al., 1991; Banister et al., 2016; Oddone et al., 2016). The RNFL thickness is compared to a built-in normative database and displayed in the RNFL thickness deviation map, which has been shown to have a high sensitivity for glaucoma detection (Leung et al., 2010; Kim et al., 2010; Ye et al., 2011; Kim et al., 2015; Shin et al., 2017). In myopia, however, the usefulness of the deviation map is limited due to a high frequency of false-positive results in healthy eyes, yielding a poor specificity (Kim et al., 2011; Leung et al., 2012; Biswas et al., 2016).

The use of separate normative data for myopic eyes has recently been suggested (Akashi et al., 2015; Biswas et al., 2016). An alternative approach could be to adjust for specific factors that are associated with both myopia and the abnormal diagnostic classification. One of these factors is the retinal blood vessel topography (Rho et al., 2014; Fujino et al., 2016). The position of the retinal blood vessels correlates strongly with the peak angle of the peripapillary RNFL (pRNFL) thickness (Yamashita et al., 2013; Pereira et al., 2014) and the retinal nerve fiber bundle trajectories (Qiu et al., 2015). Also, RNFL defects have been reported to be located along the retinal blood vessels in glaucoma suspects and patients (Hood et al., 2016). Given this close relationship between the retinal vasculature and the pRNFL thickness profile and trajectories, we hypothesize that one or more features of the retinal vasculature could be pivotal for differentiating between false-positive and true-positive glaucoma labeling in myopia.

The aim of the present study was (1) to describe the pattern of OCT abnormalities in the pRNFL deviation map in healthy myopic eyes and (2) to compare the location of the abnormalities between healthy and glaucomatous myopic eyes. For this purpose, we performed spectral-domain OCT measurements in a large group

of healthy myopic subjects and glaucoma patients. The extent and the location of the pRNFL abnormalities were depicted by the area of the color-coded region in the RNFL thickness deviation map and the location of the color-coded region relative to the location of the major temporal retinal vessels, respectively. We confirmed our observations by repeating the measurements in an independent, second study group, assessed with another type of OCT device.

Methods

Subjects

The primary study group (Group 1) consisted of 146 Chinese myopic subjects with healthy eyes and 29 Chinese patients with myopia and glaucoma. Myopia was defined as spherical equivalent (SE) ≤ -0.5 diopters. One eye per subject was included; a random eye was chosen if both eyes met the inclusion criteria. The healthy subjects were consecutively recruited from the refractive surgery clinic of the Joint Shantou International Eye Center. They received a complete ophthalmic examination including a measurement of visual acuity, intraocular pressure (IOP), perimetry (see next section), refraction, and axial length (IOL Master; Carl-Zeiss Meditec, Dublin, CA), and a dilated fundus stereoscopic examination. Subjects with best corrected visual acuity of less than 20/40, IOP over 21 mmHg, positive family history of glaucoma, previous intraocular surgery, myopic macular degeneration, glaucoma, peripapillary atrophy (PPA) extending outside the measurement circle of the OCT, refractive surgery, neurological diseases, or diabetes were excluded. For the comparison of the location of the RNFL abnormalities between false-positive healthy subjects and glaucoma patients, 29 eyes of the 29 Chinese patients with myopia and glaucoma were recruited. Glaucoma was defined as having glaucomatous optic disc damage (disc hemorrhage, notching, a vertical cup-disc ratio greater than 0.6, or an intra-individual cup-disc ratio asymmetry greater than 0.2) with corresponding repeatable glaucomatous visual field defect (see next section), regardless of the IOP level.

To validate our findings, we collected a secondary study group consisting of 122 healthy myopic eyes of 122 Chinese subjects and 79 glaucomatous eyes of 79 Chinese patients imaged with another OCT device (Group 2). The study was approved by the local ethical committee with written informed consent obtained from all subjects before participation. The present study followed the tenets of the declaration of Helsinki.

Visual field testing

Visual field testing was performed with standard automated white-on-white threshold perimetry, using the 24-2 SITA standard strategy (Humphrey Field Analyzer II; Carl Zeiss Meditec, Inc.). A visual field test was defined as reliable when fixation loss was less than 20% and false positive and false negative responses were less than 10%. The visual field tests of all the included healthy eyes had a pattern standard deviation (PSD) with P>5% and a 'within normal limits' score on the glaucoma hemifield test (GHT). All eyes with glaucoma had a repeatable visual field defect. A visual field defect was defined as a GHT score 'outside normal limits' or three or more contiguous non-edge test locations in the pattern deviation probability plot that were significantly depressed at P<0.05 with at least one test location at P<0.01, on the same side of horizontal meridian.

Optical Coherence Tomography

In the primary study group, spectral domain OCT was performed using the Cirrus High Definition OCT (software version 5.0.0.326; Carl Zeiss Meditec, Dublin, CA). The scan speed of Cirrus is 27000 A-scans per second and the axial resolution is 5 μm (Carl Zeiss 2008). We used the Optic Disk Cube 200×200 protocol for the assessment of disc area and pRNFL thickness. The real-time fundus image was used to monitor eye movements. Images with misaligned vessels within the scanning circle were excluded and retaken. All the included images had minimum signal strength of 7 (median signal strength 8).

In the secondary study group, we used the Topcon 3D OCT-2000 (software version 8.11; Topcon). The scan speed of this spectral-domain OCT is 50,000 A-scans per second and the axial resolution is 6 μm. We used the Optic Disc 3D Scan 512×128 protocol. Images with eye movements during image acquisition were excluded and retaken. All the included images had minimum image quality score of 45 as recommended by the manual.

As primary outcome measures, we analyzed the color-coded region (both yellow and red) in the RNFL thickness deviation map as provided by the devices (Carl Zeiss 2008).

Area and location of abnormalities in the RNFL thickness deviation map

We measured the area of the color coded region (both yellow and red) in the RNFL thickness deviation map. The location of the color-coded region was analyzed in eyes with a region defined as abnormal. A region was defined as abnormal in case of the presence of at least 10 (3 for Topcon OCT) contiguous yellow or red superpixels of which at least 3 (1 for Topcon OCT) superpixels within the 3.46 mm measurement circle (Kim et al., 2011). Abnormal superpixels within peripapillary atrophy were disregarded.

An abnormal region was categorized based on (1) the involved quadrant: located on the nasal, superior, inferior, or temporal quadrant and (2) the location relative to the major temporal vessels: located on the nasal side (defined as on the nasal side of both the major temporal artery and the major temporal vein) and/or on the temporal side. Thus, if any part of the color-coded region was located between the major temporal arteries and veins, the region was considered to be located on the temporal side (Figure 1). The deviation map was assessed in both the healthy and the glaucomatous eyes by two independent observers (K.P., T.K.) who were masked to the classification of the eyes. In cases of disagreement (9% of all images), the first author (K.Q.) served as an adjudicator.

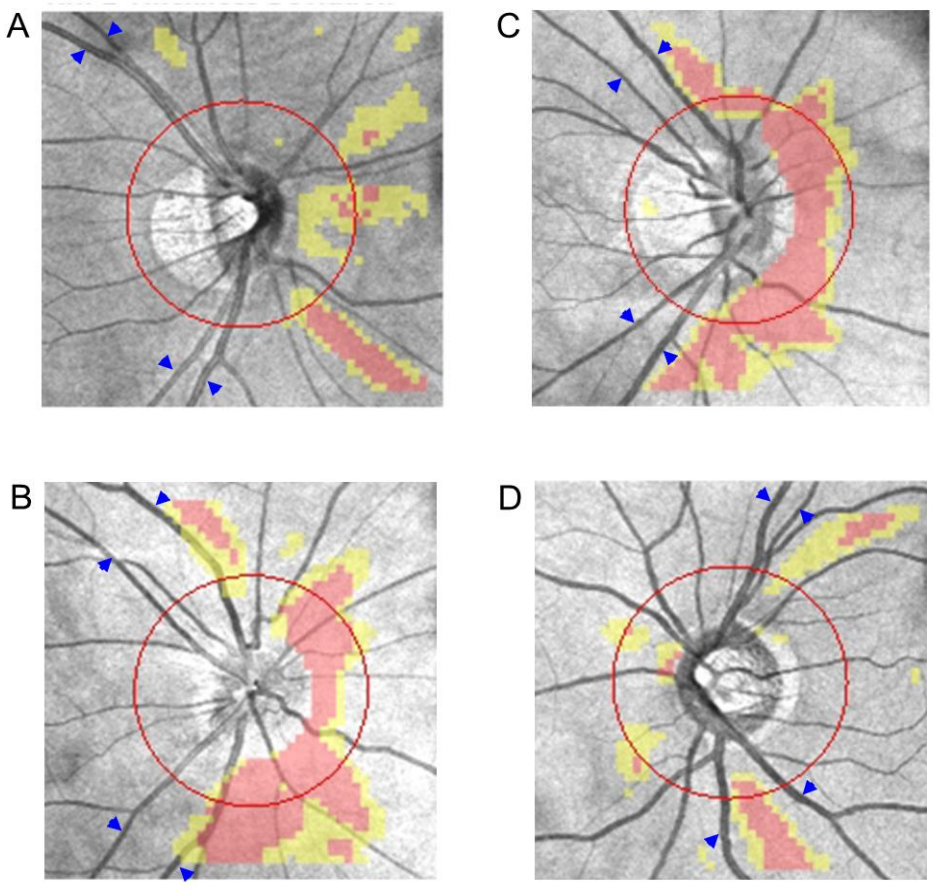

Figure 1. Characteristic patterns of the color-coded region in the RNFL thickness deviation map. A and C: Color-coded region located only on the nasal side of the major temporal arteries and veins (blue arrows); B and D: Color-coded region located at least partially on the temporal side of the major temporal arteries and veins.

Measurement of major temporal retinal blood vessel angles

The retinal vascular topography was described using the location of the major temporal retinal blood vessels. Measurements were performed with ImageJ software. Firstly, the intersections of the superotemporal artery and vein and the inferotemporal artery and vein with the 3.46 mm OCT measurement circle were manually determined by one investigator (KQ) on the OCT scanning laser ophthalmoscope image. The retinal artery angle was defined as the angle subtended by the lines joining the optic disc center and intersections between the

superotemporal/inferotemporal artery and the 3.46 mm measurement circle. The retinal vein angle was defined as the angle subtended by the lines joining the optic disc center and intersections between the superotemporal/inferotemporal vein and the 3.46 mm measurement circle.

Statistical Analysis

Differences in axial length and retinal artery angle between healthy eyes with and without a color-coded region in the RNFL thickness deviation map that qualified as abnormal were evaluated with a t-test. The associations between the area of the color-coded region and the axial length, retinal artery angle, age, and disc area (as provided by the OCT printout) were evaluated with multiple linear regression analysis.

The location of the color-coded region was quantified as the proportion of eyes with abnormalities only nasal to the main temporal vessels, and this proportion was compared between the false positives (eyes of healthy subjects with a color-coded region that qualified as abnormal) and true positives (glaucoma patients with a color-coded region that qualified as abnormal), using a chi-square test with Yates correction. The sensitivity and specificity of glaucoma detection with OCT were calculated for a positive test result defined as (1) the presence of a color-coded region in the deviation map that qualified as abnormal (Criterion 1) and (2) the presence of a color-coded region in the deviation map that qualified as abnormal and was located at least partially on the temporal side of the major temporal retinal vessels (Criterion 2). As a reference, we also calculated the specificity of a common OCT parameter, the Average RNFL thickness, at a sensitivity similar to that of our Criterion 2. Sensitivity and specificity corresponding to these two criteria and to the average RNFL thickness were compared with a McNemar test. A P value of 0.05 or less was considered statistically significant. The statistical analyses were performed with SPSS software (version 17.0; SPSS Inc, Chicago, IL).

Results

In Group 1, 9 healthy subjects were excluded because of unreliable visual field tests (7 subjects) and PPA extending outside the OCT measurement circle (2 subjects); 4 glaucoma patients were excluded because of poor image quality OCT scans. Finally, 137 (146-9) healthy eyes of 137 myopic subjects (63 females and 88 right eyes) and 25 glaucomatous eyes of 25 patients (9 females and 13 right eyes) were included in the analysis. In Group 2, after excluding 6 healthy subjects (unreliable visual field tests) and 5 glaucoma patients (poor image quality OCT scans), 116 healthy eyes of 116 myopic subjects and 74 glaucomatous eyes (41 eyes had SE ≤ -0.5 diopters) of 74 glaucoma patients were included. Table 1 shows the demographics of the two study populations. Glaucomatous eyes had a significantly larger artery angle and vein angle than the healthy eyes, in both study groups (both $P<0.001$), but this difference disappeared after adjustment for axial length.

In the 137 healthy eyes of Group 1, the median (inter-quartile range [IQR]) area of the color-coded region in the deviation map was 1.8 (0.7 to 3.4) mm^2. The color-coded region was qualified as abnormal in 106 (77.4%) of these eyes (false positives). This was the case in 24 of the 25 (96%) glaucomatous eyes of Group 1 (true positives). The 106 false-positive healthy eyes had a greater axial length (25.8 ± 1.1 versus 25.2 ± 1.0 mm; P=0.017) and a smaller retinal artery angle (130 ± 17° versus 141 ± 16°; P=0.002) compared to the remaining 31 healthy eyes without a color-coded region that qualified as abnormal (true negatives). In the multivariable analysis (adjusted for age and disc area), both axial length (beta=0.37 mm^2/mm; $P<0.001$) and artery angle (beta=-0.24 mm^2/deg; P=0.004) were significantly associated with the area of the color-coded region.

Table 1. Characteristics of the primary (137 healthy and 25 glaucomatous eyes) and secondary (116 healthy and 74 glaucomatous eyes) study group

	Primary study group (Group 1)				**Secondary study group (Group 2)**			
	Healthy eyes		Glaucomatous eyes		Healthy eyes		Glaucomatous eyes	
	Median (IQR)	Range	Median (IQR)	Range	Median (IQR)	Range	Median (IQR)	Range
Age, y	22.2 (20.1 to 24.0)	18 to 40	41.6 (29.9 to 60.7)	23 to 68	31.2 (25.0 to 42.0)	21 to 70	50.0 (37.0 to 62.0)	20 to 77
Spherical equivalent, D	-4.88 (-6.75 to -3.69)	-15.75 to -0.5	-4.55 (-7.00 to -1.00)	-17.75 to -0.75	-3.00 (-4.25 to -2.00)	-0.50 to -8.50	-2.00 (-3.50 to 0.50)	-6.75 to 2.50
Axial length, mm	25.6 (24.9 to 26.3)	22.5 to 28.8	25.3 (24.2 to 26.4)	22.4 to 28.3	24.3 (23.6 to 25.2)	21.5 to 28.1	23.8 (23.4 to 24.6)	22.1 to 28.5
MD, dB	-2.1 (-2.7 to -1.5)	-4.9 to 1.5	-14.4 (-27.1 to -7.2)	-32.0 to -3.4	-0.9 (-1.9 to -0.3)	-4.2 to 1.2	-10.2 (-14.6 to -4.0)	-29.5 to -1.3
Average RNFL thickness, μm	99.0 (91.0 to 103.5)	81.0 to 128.0	62.8 (55.0 to 78.3)	48.0 to 107.0	108.0 (102.0 to 112.0)	84.0 to 126.0	77.0 (66.0 to 89.0)	49.0 to 123.0
Retinal artery angle, deg	132 (121 to 145)	71 to 173	139 (131 to 146)	92 to 168	135 (122 to 148)	75 to 170	140 (125 to 155)	78 to 169
Retinal vein angle, deg	137 (121 to 152)	92 to 190	148 (129 to 162)	113 to 179	139 (124 to 155)	93 to 191	142 (126 to 160)	98 to 193

Among the 106 false-positive healthy eyes of Group 1, 64 eyes (60.4%) had the color-coded region located in the inferior and/or superior region. These 64 eyes had a greater axial length (26.1 ± 1.1 versus 25.2 ± 1.0 mm; P<0.001) and a smaller retinal artery angle (121 ± 19° versus 133 ± 11°; P=0.002) compared to the remaining 42 eyes with only nasal involvement. Figure 2 illustrates this association between the color-coded region, axial length, and retinal artery angle. Among the 64 healthy eyes with inferior and/or superior region color coding, 53 eyes (82.8%) had the color coding expanding to the superotemporal (11 o'clock in right-eye orientation) and/or inferotemporal (7 o'clock in right-eye orientation) region (Figures 1B and C), which are the specific regions where RNFL defects are commonly observed in glaucomatous eyes. In these 53 eyes, however, 48 (90.6%) eyes had the color-coded region located only on the nasal side of the major temporal retinal vessels – related to the associated small arterial angle (Figure 2 A-D). In total, 101 of 106 (95.3%) false-positive healthy myopic eyes had the color-coded region located only on the nasal side of the major temporal retinal vessels. Interestingly, none of the 24 true-positive glaucomatous eyes had the color-coded region located only on the nasal side of the major temporal retinal vessels (101 of 106 versus 0 of 24; P<0.001). This is illustrated in Figure 3A (healthy eye) and Figure 3B (glaucoma). When a positive test result was defined as the presence of a color-coded region that qualified as abnormal (Criterion 1), the sensitivity and specificity were 96 and 22.6%, respectively. By additionally requiring that the color-coded region had to be located at least partially on the temporal side of the major temporal retinal vessels (Criterion 2), the specificity increased dramatically to 96.4% (96.4 versus 22.6%, P<0.001) without any decrease in sensitivity (Table 2A).

In Group 2, 44 of 116 healthy myopic eyes (37.9%) and 70 of 74 glaucomatous eyes (94.6%) had a color-coded region that qualified as abnormal in the deviation map. Of the 44 false-positive healthy myopic eyes, 37 eyes (84.1%) had the color-coded region located only on the nasal side of the major temporal retinal vessels. Among the 70 true-positive glaucomatous eyes, only 2 eyes (2.9%) had the color-coded region located only on the nasal side of the major temporal retinal vessels

(37 of 44 versus 2 of 70; P<0.001). This is illustrated in Figure 3C (healthy eye) and Figure 3D (glaucoma). Thus, also in this study group and OCT device, additionally requiring that the color-coded region had to be located at least partially on the temporal side of the major temporal retinal vessels yielded a substantial increase in specificity (94.0 versus 61.2%, P<0.001) without a significant decrease in sensitivity (Table 2B).

Table 2. Sensitivity and specificity of OCT for the two definitions of a positive test result based on the area (Criterion 1) and the area and location (Criterion 2) of the color-coded region in the RNFL thickness deviation map

	Sensitivity (95%CI)	Specificity (95%CI)
A: Primary study group		
Criterion 1	96.0% (77.7 to 99.8%)	22.6% (16.1 to 30.7%)
Criterion 2	96.0% (77.7 to 99.8%)	96.4% (91.3 to 98.6%)
P value	1.0	<0.001
B: Secondary study group		
Criterion 1	94.6% (82.0 to 98.3%)	62.1% (52.6 to 70.8%)
Criterion 2	91.9% (82.6 to 96.7%)	94.0% (87.5 to 97.3%)
P value	0.65	<0.001

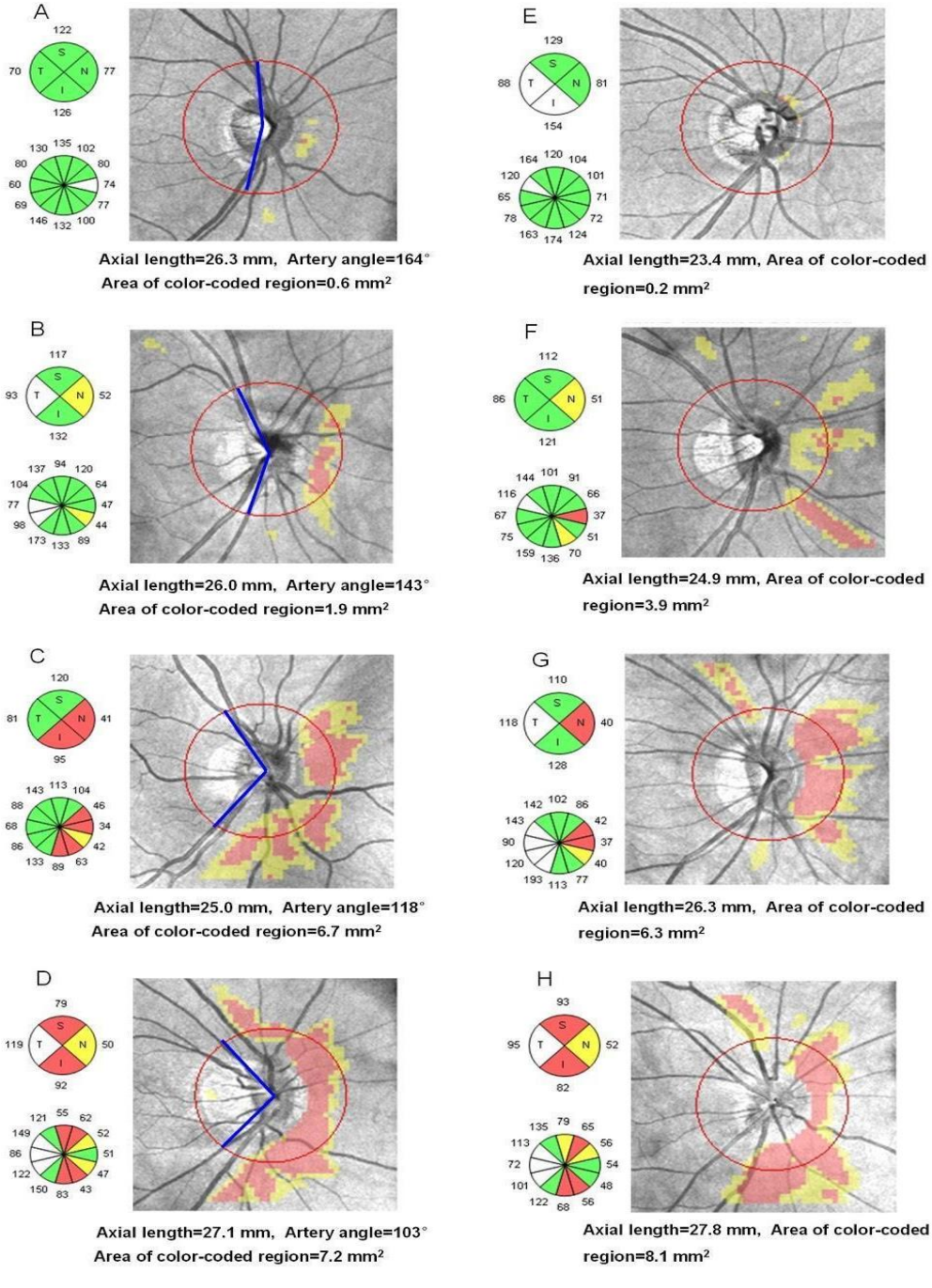

Figure 2. Cases demonstrating the association between the artery angle (left column, A to D) and axial length (right column, E to H) and the color-coded region in the RNFL thickness deviation map.

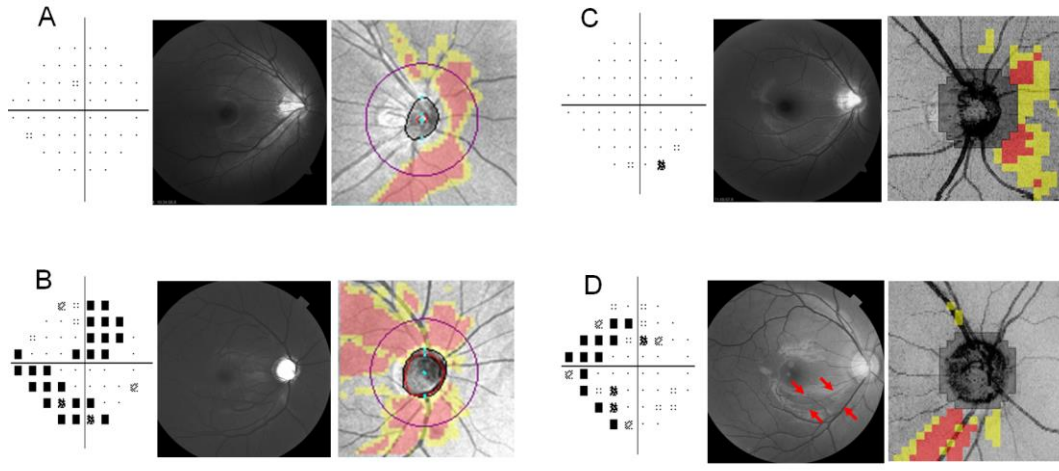

Figure 3. Patterns of false-positive color-coded regions (A and C, healthy eyes) and glaucomatous RNFL defects (B and D, glaucomatous eyes) in four cases imaged with Cirrus OCT (A and B) and Topcon OCT (C and D). Of note, the color-coded region in healthy myopic eyes (A and C) are located only on the nasal side of the major temporal vessels whereas RNFL defects in glaucomatous eyes are located on the temporal side (D; localized RNFL defect [red arrows]; visual field mean deviation -4 dB) or expanding to the nasal side (B; diffuse RNFL defect; mean deviation -13 dB).

In order to compare the diagnostic performance of our Criterion 2 to the common OCT parameter Average RNFL thickness, we compared specificities at a balanced sensitivity. For the Criterion 2 sensitivities of 96.0 and 91.2% for Group 1 and Group 2, respectively (Table 2), this resulted for Average RNFL thickness in a specificity of 39.4% for Group I (to be compared to 96.4% for Criterion 2; $P<0.001$) and of 78.5% for Group 2 (to be compared to 94.0%; $P<0.001$).

Finally, our location criterion can also be combined with the OCT parameter Average RNFL thickness. Average RNFL thickness has, at a sensitivity of 95%, a specificity of 41.2% in Group 1 and of 62.4% in Group 2. By additionally requiring abnormalities in the deviation map on the temporal side of the major vessels, the specificity increased from 41.2% to 96.4% in Group 1 ($P<0.001$) and from 62.4% to 95.7% in Group 2 ($P<0.001$) without a noticeable change in sensitivity (sensitivity dropped from 95% to 94 and 93%, respectively).

Discussion

The characteristic location of the color-coded region in the RNFL thickness deviation map of healthy myopic eyes, being exclusively on the nasal side of the major temporal retinal vessels, yields an opportunity to differentiate between glaucoma and false-positive labeling. Analysis of the characteristic location of the color-coded region in the thickness deviation map significantly improves the diagnostic performance compared to the common OCT parameter Average RNFL thickness.

In the present study, eyes with a smaller retinal artery angle (horizontally deviated blood vessels) were associated with a greater area of the color-coded region in the deviation map. A possible explanation for this finding is the close association between retinal vasculature and the RNFL profile (Eichmann et al.,2005; Dorrell & Friedlander 2006; Yamashita et al., 2013; Pereira et al., 2014; Resch et al., 2015). In eyes with a small artery angle, the RNFL thickness profile tends to shift to the temporal region causing a different distribution of the RNFL thickness (relatively thick RNFL thickness in the temporal region and relatively thin RNFL thickness in the superior and inferior region). As the normative database does not consider the variation of the retinal vasculature, one would not be surprised to find a false-positive classification in the inferior and superior quadrants in eyes with a small artery angle (see Fig. 2). On the other hand, an RNFL defect located in the temporal region of an eye with a small artery angle may be overlooked by the device (because it is still within the allowed range according to the normative database). Indeed, temporally located RNFL defects as identified with red-free fundus photography were reported to be often overlooked in the OCT deviation map (Hwang et al., 2013). Consistent with previous studies (Kim et al., 2011; Leung et al., 2012; Kim et al., 2015; Qiu et al., 2011), we found that a longer axial length was significantly associated with the area of the color-coded region in the deviation map.

Previously, high percentages of false-positive test results in the RNFL thickness deviation map have been observed in myopic eyes (Leung et al., 2012; Biswas et al., 2015). In agreement with these studies, we found that three quarters of the healthy myopic eyes were classified as abnormal in the RNFL deviation map of Cirrus HD OCT. In view of the high false-positive rate in myopic eyes, it is important to differentiate glaucomatous RNFL defects from false-positive abnormalities in clinical practice. The characteristics of glaucomatous RNFL defects have been described before (Kimura et al., 2012; Hwang et al., 2014). Briefly, the glaucomatous RNFL defects in the peripapillary area are predominantly located in the superotemporal and/or inferotemporal region for early stage glaucoma (Figure 3D) and expand to the superonasal and/or inferonasal region for more advanced disease (Figure 3B). In the current study, eyes with smaller artery angles tended to have color-coded regions located in the superotemporal and/or inferotemporal region (the similar regions in which typical glaucomatous RNFL defects are commonly observed), making it difficult to differentiate between glaucoma and false-positive labeling. However, we found that the vast majority of the false-positive healthy myopic eyes had the color-coded region located only on the nasal side of the major temporal retinal vessels (Figure 2A-G; Figure 3A, C). In contrast, none of the glaucomatous eyes with a color-coded region had the color-coded region located only on the nasal side of the major temporal retinal vessels. By taking this important, characteristic feature into account, we were able to increase the specificity significantly without sacrificing the sensitivity (Table 2A; validated in another study group with another OCT device [Table 2B]). Our findings suggest that the location of the color-coded region in the RNFL deviation map relative to the major temporal retinal vessels offers a valuable clue for differentiating between glaucoma and false-positive labeling in myopic eyes.

The reason why the relative location of RNFL defects (that is, relative to the major temporal vessels) is more important than the absolute location remains unclear. A possible explanation is the close relationship between the RNFL profile and the major retinal blood vessels. RNFL defects have been reported to

be located along the retinal blood vessels in glaucoma suspects and patients (Hood et al., 2016). Another possible explanation is that retinal blood vessels tend to nasalize in glaucomatous eyes (Varma et al., 1987; Radcliffe et al., 2014), which could contribute to the typical location of RNFL defects in glaucoma, being at least partly on the temporal side of the major blood vessels. Previously, it has been reported that shifting the normative database according to vessel position strengthens the structure–function relationship and improves the diagnostic performance regarding the RNFL profile (Rho et al., 2014; Fujino et al., 2016). The changing vessel position might complicate the use of such a database in longitudinal studies or progression detection in clinical care.

There are limitations in the present study. One limitation of this study was that the subjects were all Chinese and of a limited age range. A population-based study including subjects with different ethnicities and ages is needed to allow for a generalization of our findings. Cases and controls differed by age. However, all parameters used in this study are age-corrected, as they are based on comparisons with a normative database that includes age. Another limitation is the cross-sectional nature of the present study. Some eyes with subclinical glaucomatous damage may have been included in the current analysis. We tried to avoid this as much as possible by applying strict inclusion and exclusion criteria. Future longitudinal studies are needed to confirm our results. Strength of the present study is the fact that our main finding (improvement in specificity) is not only statistically significant, but also - due to the large effect - highly clinically relevant.

In summary, significant inter-individual variations exist in the trajectories of the major temporal retinal vessel in healthy myopic eyes. Especially eyes with a small artery angle are prone to a false-positive glaucoma classification. The location of the color-coded region relative to the major temporal retinal vessels offers a valuable clue for differentiating between false-positive and glaucoma in myopic eyes.

References

Akashi A, Kanamori A, Ueda K, Inoue Y, Yamada Y, Nakamura M. The Ability of SD-OCT to Differentiate Early Glaucoma With High Myopia From Highly Myopic Controls and Nonhighly Myopic Controls. Invest Ophthalmol Vis Sci. 2015 Oct;56(11):6573-6580.

Banister K, Boachie C, Bourne R, et al. Can Automated Imaging for Optic Disc and Retinal Nerve Fiber Layer Analysis Aid Glaucoma Detection? Ophthalmology. 2016 May;123(5):930-938.

Biswas S, Lin C, Leung CK. Evaluation of a Myopic Normative Database for Analysis of Retinal Nerve Fiber Layer Thickness. JAMA Ophthalmol. 2016 Sep 1;134(9):1032-1039.

Carl Zeiss Meditec, Inc. Cirrus HD-OCT User Manual. Dublin, CA: Carl Zeiss Meditec, Inc.; 2008;4.18-9. Rev. A.

Dorrell MI, Friedlander M. Mechanisms of endothelial cell guidance and vascular patterning in the developing mouse retina. Prog Retin Eye Res. 2006;25:277-295.

Eichmann A, Makinen T, Alitalo K. Neural guidance molecules regulate vascular remodeling and vessel navigation. Genes Dev. 2005;19:1013-1021.

Fujino Y, Yamashita T, Murata H, Asaoka R. Adjusting Circumpapillary Retinal Nerve Fiber Layer Profile Using Retinal Artery Position Improves the Structure-Function Relationship in Glaucoma. Invest Ophthalmol Vis Sci. 2016 Jun 1;57(7):3152-3158.

Hood DC, De Cuir N, Mavrommatis MA, et al. Defects Along Blood Vessels in Glaucoma Suspects and Patients.Invest Ophthalmol Vis Sci. 2016 Apr;57(4):1680-1686.

Huang D, Swanson EA, Lin CP, et al. Optical coherence tomography. Science. 1991;254(5035):1178-1181.

Hwang YH, Kim YY, Kim HK, Sohn YH. Ability of cirrus high-definition spectral-domain optical coherence tomography clock-hour, deviation, and thickness maps in detecting photographic retinal nerve fiber layer abnormalities. Ophthalmology. 2013 Jul;120(7):1380-1387.

Hwang YH, Kim YY, Kim HK, Sohn YH. Agreement of retinal nerve fiber layer defect location between red-free fundus photography and cirrus HD-OCT maps. Curr Eye Res. 2014 Nov;39(11):1099-1105.

Kim KE, Jeoung JW, Park KH, Kim DM, Kim SH. Diagnostic classification of macular ganglion cell and retinal nerve fiber layer analysis: differentiation of false-positives from glaucoma. Ophthalmology. 2015 Mar;122(3):502-510.

Kim MJ, Park KH, Yoo BW, Jeoung JW, Kim HC, Kim DM. Comparison of macular GCIPL and peripapillary RNFL deviation maps for detection of glaucomatous eye with localized RNFL defect. Acta Ophthalmol. 2015 Feb;93(1):e22-28.

Kim NR, Lee ES, Seong GJ, Choi EH, Hong S, Kim CY. Spectral-domain optical coherence tomography for detection of localized retinal nerve fiber layer defects in patients with open-angle glaucoma. Arch Ophthalmol. 2010 Sep;128(9):1121-1128.

Kim NR, Lim H, Kim JH, Rho SS, Seong GJ, Kim CY. Factors associated with false positives in retinal nerve fiber layer color codes from spectral-domain optical coherence tomography. Ophthalmology. 2011 Sep;118(9):1774-1781.

Kimura Y, Hangai M, Morooka S, et al. Retinal nerve fiber layer defects in highly myopic eyes with early glaucoma. Invest Ophthalmol Vis Sci. 2012 Sep 21;53(10):6472-6478.

Leung CK, Lam S, Weinreb RN, et al. Retinal nerve fiber layer imaging with spectral-domain optical coherence tomography: analysis of the retinal nerve fiber layer map for glaucoma detection. Ophthalmology. 2010 Sep;117(9):1684-1691.

Leung CK, Yu M, Weinreb RN, et al. Retinal nerve fiber layer imaging with spectral-domain optical coherence tomography: interpreting the RNFL maps in healthy myopic eyes. Invest Ophthalmol Vis Sci. 2012 Oct 17; 53(11): 7194-7200.

Oddone F, Lucenteforte E, Michelessi M, et al. Macular versus Retinal Nerve Fiber Layer Parameters for Diagnosing Manifest Glaucoma: A Systematic Review of Diagnostic Accuracy Studies. Ophthalmology. 2016 May;123(5):939-949.

Pereira I, Weber S, Holzer S, et al. Correlation between retinal vessel density profile and circumpapillary RNFL thickness measured with Fourier-domain optical coherence tomography. Br J Ophthalmol. 2014 Apr; 98(4): 538-543.

Qiu K, Schiefer J, Nevalainen J, Schiefer U, Jansonius NM. Influence of the Retinal Blood Vessel Topography on the Variability of the Retinal Nerve Fiber Bundle Trajectories in the Human Retina. Invest Ophthalmol Vis Sci. 2015 Oct;56(11):6320-6325.

Qiu KL, Zhang MZ, Leung CK, et al. Diagnostic classification of retinal nerve fiber layer measurement in myopic eyes: a comparison between time-domain and spectral-domain optical coherence tomography. Am J Ophthalmol. 2011 Oct;152(4):646-653.e2.

Radcliffe NM, Smith SD, Syed ZA, Park SC, Ehrlich JR, De Moraes CG, Liebmann JM, Ritch R.Retinal blood vessel positional shifts and glaucoma progression. Ophthalmology. 2014 Apr;121(4):842-848.

Resch H, Pereira I, Weber S, Holzer S, Fischer G, Vass C. Retinal Blood Vessel Distribution Correlates With the Peripapillary Retinal Nerve Fiber Layer Thickness Profile as Measured With GDx VCC and ECC. J Glaucoma. 2015 Jun-Jul; 24(5): 389-395.

Rho S, Sung Y, Kang T, Kim NR, Kim CY. Improvement of diagnostic performance regarding retinal nerve fiber layer defect using shifting of the normative database according to vessel position. Invest Ophthalmol Vis Sci. 2014 Jul 29;55(8):5116-5124.

Shin JW, Seong M, Lee JW, Hong EH, Uhm KB. Diagnostic Ability of Retinal Nerve Fiber Layer Thickness Deviation Map for Localized and Diffuse Retinal Nerve Fiber Layer Defects. J Ophthalmol. 2017;2017:8365090.

Varma R, Spaeth GL, Hanau C, Steinmann WC, Feldman RM. Positional changes in the vasculature of the optic disk in glaucoma.Am J Ophthalmol. 1987 Nov 15;104(5):457-464.

Yamashita T, Asaoka R, Tanaka M, et al. Relationship between position of peak retinal nerve fiber layer thickness and retinal arteries on sectoral retinal nerve fiber layer thickness. Invest Ophthalmol Vis Sci. 2013;54:5481-5488.

Ye C, To E, Weinreb RN, et al. Comparison of retinal nerve fiber layer imaging by spectral domain optical coherence tomography and scanning laser ophthalmoscopy. Ophthalmology. 2011 Nov;118(11):2196-2202.